(Lectures given at the "Ettore Majorana Int'l Summer School," Erice, Sicily, July 1969.)

SLAC-PUB-689
December 1969
(TH) and (EXP)

INELASTIC ELECTRON SCATTERING, ASYMPTOTIC BEHAVIOR, AND SUM RULES*

S. D. Drell

Stanford Linear Accelerator Center
Stanford University, Stanford, California 94305

Electron scattering from a hadron target has a singularly attractive feature relative to the various processes of hadrons scattering from hadron targets: the electromagnetic field generated during the electrons's scattering is understood if indeed anything is in particle physics. Dirac tells us the transition current of the scattered electron and Maxwell tells us the rest. Therefore, in this process we are probing the structure of the hadron by means of a known operator — the electromagnetic current operator. There is an additional advantage in studying this process and that is its weakness. We can do our theoretical analyses to lowest order in the fine structure constant $\alpha \approx 1/137$ which is a comfortable expansion parameter for quantitative results.

The first detailed high energy experimental studies of electron scattering from hydrogen targets concentrated on the elastic process

$$e + p \longrightarrow e' + p'$$

and measured the elastic form factors defined by

$$\langle \underline{P}' \left| J_\mu \right| \underline{P} \rangle = \left(\sqrt{\frac{M^2}{(2\pi)^6 EE'}} \right) \bar{u}(p') \left[\gamma_\mu F_1(q^2) + \frac{i\sigma_{\mu\nu} q^\nu}{2M} \kappa F_2(q^2) \right] u(p) \qquad (1)$$

*Work supported by the U. S. Atomic Energy Commission.

where J_μ is the Heisenberg current operator, $|P\rangle$ and $|P'\rangle$ denote physical proton states of momenta (E, $\underline{P}$) and (E', $\underline{P}'$) respectively, and the Dirac and Pauli form factors F_1 and F_2 are functions of the invariant momentum transfer $q^2 = (p - p')^2 = (E - E')^2 - (\underline{P} - \underline{P}')^2 = 2M^2 - 2P\cdot P' < 0$. The observed rapid fall-off of the magnetic form factor for the proton which decreases roughly as $\left(\frac{1}{q^2}\right)^2$ for large q^2 from several to $\cong 25$ $(\text{GeV})^2$, coupled with the theoretically popular scaling law[1]

$$\frac{G_M(q^2)}{G_E(q^2)} = \frac{F_1(q^2) + \kappa F_2(q^2)}{F_1(q^2) + \kappa \frac{q^2}{4M^2} F_2(q^2)} = 2.79$$

allows us to write simply for the ratio of electron-proton scattering to its theoretical value for a point proton (with the observed magnetic moment):

$$\left(\frac{d\sigma}{d\Omega}\right)_{\text{exptl}} \simeq \left(\frac{d\sigma}{d\Omega}\right)_{\text{point}} \times \left(\frac{1}{q^2}\right)^4 \text{ for } -q^2 > \text{several } (\text{GeV})^2. \tag{2}$$

For elastic scattering the momentum transfer to the proton, q^2, and the energy transfer $q \cdot P \equiv M\nu$, with ν the energy transfer computed in the target proton's rest system, are related by the mass shell condition

$$(q + P)^2 = M^2 = M^2 + q^2 + 2M\nu \tag{3}$$

or $2M\nu = -q^2$.

Moving next to inelastic scattering with the excitation of particular proton resonances the matrix element (1) is replaced by

$$\langle P'_{\text{res}} | J_\mu | P \rangle$$

and the mass shell condition (3) by

$$(q + P)^2 = M^2_{\text{res}} = M^2 + q^2 + 2M\nu$$

or

$$2M\nu = -q^2 + (M^2_{\text{res}} - M^2).$$

The kinematic region in the (q^2, $2M\nu$) plane is thus displaced by a constant increasing with the mass of the resonance being formed. Once again experiment[2] indicates a very rapid decrease in the cross section for such excitations that roughly parallels the rapid decrease in (2) for the elastic process.

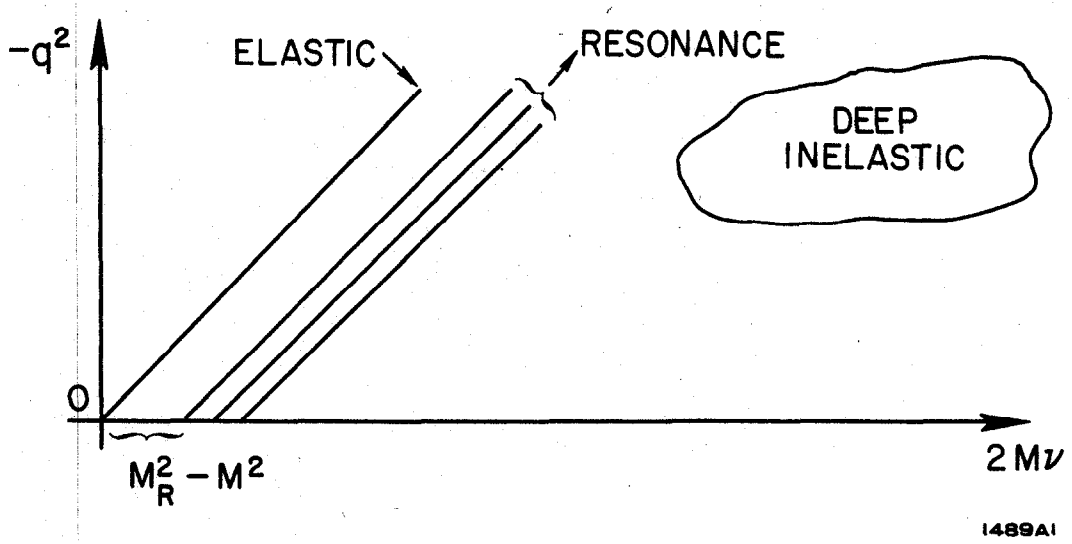

FIG. 1

The next step in the evolution of studies of electron-proton scattering is to look at very inelastic scattering — i.e., the continuum region beyond the elastic and "discrete" resonance excitations in Fig. 1. In the analogous process of atomic scattering of electrons, beyond the elastic process leaving the atom in its ground state and the excitation of discrete atomic levels by inelastic scattering there is the continuum of inelastic processes ionizing the atom. Similarly electron scattering from nuclei can be elastic, can lead to excited nuclear levels, or can disintegrate the nucleus by ejecting individual nucleons analogous to the atomic ionization. Here we shall be interested in the "pionization" of the proton — i.e., the deep inelastic region in the continuum beyond the elastic and resonance contours shown in Fig. 1.

In the deep inelastic scattering region we are interested in the behavior of the proton's structure functions as a function of the momentum transfer q^2, the energy transfer $2M\nu > -q^2$, and the particular hadron channels $|\overline{X}>$ being populated by $<\overline{X}\,|J_\mu|\,P>$. In these lectures we will focus on sum rule type measurements which detect only the final electron scattered through a given angle θ with momentum and energy transfers q^2 and $2M\nu$ and sum over all final hadron channels. In order to help anticipate and interpret the behavior of the proton's structure functions as measured in this way we refer back to the nuclear physics analogue for a useful if imperfect guide.

The big difference between the proton and nuclei or atoms is that the latter are structures made up of weakly bound and well identified individual nucleons or electrons. Thus the ratio of binding energies to rest energies for the constituents are typically

for an atom $\quad \dfrac{\text{few eV}}{.51\ \text{MeV}} \sim 10^{-5} \ll 1$

for a nucleus $\quad \dfrac{8\ \text{MeV}}{938\ \text{MeV}} \sim 10^{-2} \ll 1$

for a proton $\quad \dfrac{\text{100's of MeV}}{\text{100's of MeV}} \sim 1\,.$

Associated with their strong binding is the fact that the constituents of a proton remain elusive enigmas of unknown numbers (finite?) as well as unknown qualitative properties like charge, spin, and mass. In contrast there is no uncertainty as to the numbers and identity of nucleons and electrons forming a nucleus or an atom.

In view of these comments we are well aware of the fact that nuclei and atoms provide but an imperfect analogy to help guide us in the study of the deep inelastic electron-proton scattering (and the related processes of deep inelastic electron-positron annihilation and of neutrino-inelastic scattering). They are, however, also useful analogies to turn to — in particular in search of simplifying kinematic regions and general features.

Consider in particular inelastic-electron scattering from a nucleus with A nucleons and Z protons each treated as very massive so that we take into account only the static Coulomb interaction. The transition amplitude is then

$$A \sim \frac{e^2}{q^2} \langle \underline{\overline{X}} \left| \sum_{\text{protons}} e^{i\underline{q} \cdot \underline{r}_p} \right| \underline{P}_{\underline{z}A} \rangle \tag{4}$$

and the differential cross section derived by standard steps is

$$\frac{d^2\sigma}{d|\vec{q}|^2 d\nu} = \frac{4\pi\alpha^2}{|q|^4} \sum_{\underline{\overline{X}}} \delta(E_p + \nu - E_x) \langle \underline{P} \left| \sum_i e^{-i\underline{q} \cdot \underline{r}_i} \right| \underline{\overline{X}} \rangle \langle \underline{\overline{X}} \left| \sum_j e^{i\underline{q} \cdot \underline{r}_j} \right| \underline{P} \rangle \tag{5}$$

where the sums over i and j include all protons and the sum on $\underline{\overline{X}}$ is over all nuclear states satisfying the energy conserving δ–function $E_x = E_p + \nu$.

Summing over all energy transfers ν for fixed momentum transfer $|\underline{q}|^2$ we can use closure to construct a sum rule free of reference to the specific final hadron states[3]

$$\int_{|q|^2 \text{ const.}} d\nu \frac{d^2\sigma}{d|q^2|d\nu} = \frac{4\pi\alpha^2}{|\underline{q}|^4} \langle \underline{P} \left| \sum_{i,j} e^{i\underline{q} \cdot (\underline{r}_i - \underline{r}_j)} \right| \underline{P} \rangle = \frac{4\pi\alpha^2}{|\underline{q}|^4} \left\{ Z + Z(Z-1) f_2(|q|^2) \right\} \tag{6}$$

where f_2 is the two-body correlation function.

Equation (6) is the Heisenberg generalization of the Thomas-Reiche-Kuhn dipole sum rule first derived for evaluating the f-numbers for the atomic photo-electric effect. From (5) and (6) we draw several observations for our present discussion: For q sufficiently large the two body correlation function vanishes. Generally f_2 is small for $q > \{\text{Mean inter-nucleon separation}\}^{-1} \sim 150$ MeV in which case

$$\frac{d\sigma}{d|\underline{q}|^2} \longrightarrow \frac{4\pi\alpha^2}{|\underline{q}|^4} Z \qquad \text{for } q \geq 200 \text{ MeV} \tag{7}$$

This tells us that there is a finite area under the inelastic scattering curve including all final continuum states of the nucleus and at a fixed and large momentum transfer

q from the electron. In contrast the differential cross sections to individual excited nuclear states vanish rapidly in analogy with the proton results. However, (7) tells us that the total area at fixed q is just the point scattering result $\left\{4\pi(Z\alpha)^2/|q|^4\right\}$ multiplied by 1/Z, or the reciprocal of the number of point charges constituting a nucleus. This factor enters because (6) is proportional to the sum of the squares of the elementary proton charges whereas for a point target and elastic scattering all the charges scatter coherently and the cross section is proportional to the square of the sum of the charges. Recall that we are working in a range of q values where the effects of meson production, exchange currents, retardation corrections to Coulomb scattering, etc., may be ignored and the proton may be treated as a point charge. Another way of looking at (7) is to observe that it corresponds to scattering from Z independent and incoherent point Coulomb scatterers. It is the same result as the impulse approximation treatment of scattering by each individual proton in the nucleus.

The correlations and binding forces in the nucleus are negligible and the protons can be treated as approximately free in this kinematical region. The area under the curve in (7) counts the number of elementary point constituents of unit charge of the nucleus and is independent of all dynamical details. Can we infer the same for the proton?

We can learn more from the spectrum of the inelastic-electron scattering curve as illustrated in the Fig. 2 schematically representing what happens for large q. There is a peak in the continuum inelastic scattering curve at an energy loss corresponding to quasi-elastic scattering from a single nucleon. This quasi-elastic peak occurs at

$$\nu_{qe} \cong |\underline{q}|^2/2M = \left[|\underline{q}|^2/2(AM)\right] A \qquad (8)$$

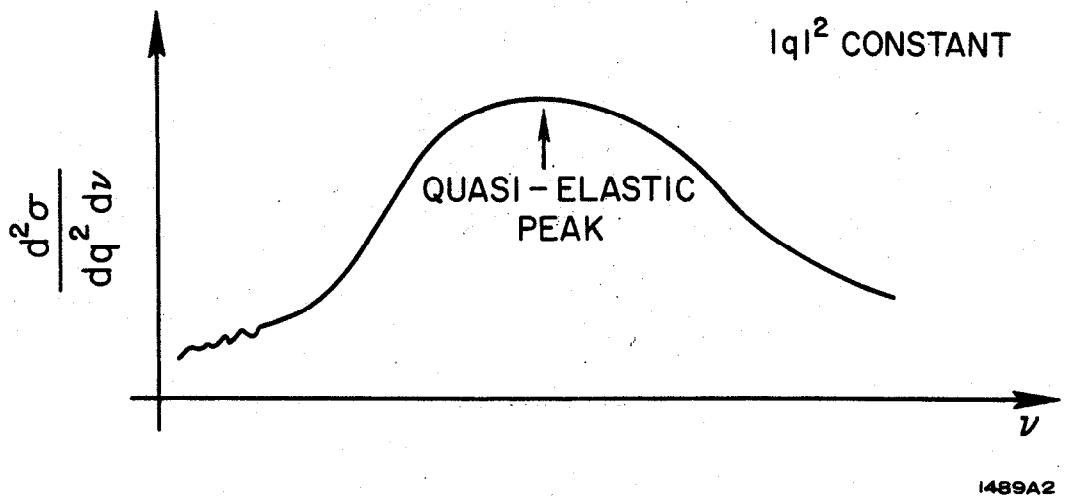

FIG. 2

telling us that each constituent has a mass that is (1/A) of the total nuclear mass. This peak is broadened by the Fermi motion of the nucleons inside of the nucleus. Thus a quasi-elastic peak in the deep inelastic continuum from a proton would reveal the mass of the proton's constituents, if this is well defined and is not obscured by large Fermi momenta, by a relation such as (8) made suitably relativistic.

Returning now to the fully relativistic problem of scattering from the proton we look first for a kinematic region where a simple general sum rule such as (7) can be constructed free of all dynamical details. We look in other words for the kinematic conditions that are appropriate for applying an impulse approximation. This suggests that we look in the region of large values of momentum transfer $q^2 = -Q^2 < 0$ and large energy transfers ν so that the interaction can be treated as a sudden pulse. During the brief duration of this pulse the constituents – or "partons" – of the nucleon can be treated as instantaneously free so that an impulse approximation will be valid.

Following the original intuitive arguments of Feynman[4] we construct the criterion for applying the impulse approach and viewing the proton as an assemblage of "free" or "long lived" partons. In terms of the language of old-fashioned perturbation theory and of the uncertainty principle we want the energy transfer from the electron to the proton, q_0, to be larger than the transition frequencies or energy differences, ΔE, between the important component states that couple together to form the physical proton — i.e.,

$$1/\tau_{\text{interaction}} \sim q_0 \gg \Delta E \tag{9}$$

To establish the conditions for (9) to apply let us work in the center-of-mass system of the colliding high energy incident electron plus proton. With the four momenta as illustrated in Fig. 3

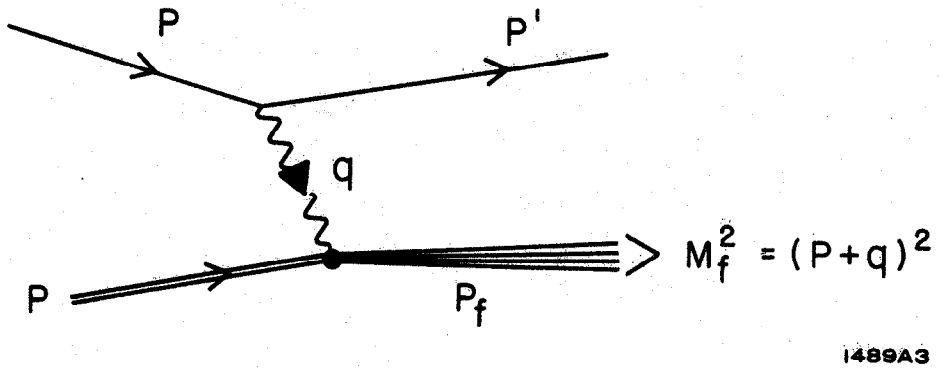

FIG. 3

we have, with the collision along the 3 axis and $M/P \longrightarrow 0$: $p = (P,\ 0,\ 0,\ -P)$, $P = \left(P + \frac{M^2}{2P},\ 0,\ 0,\ P\right)$ and:

$$\begin{cases} q_0 = (2M\nu - Q^2)/4P \\ q_3 = -(2M\nu + Q^2)/4P \\ q^2 = -Q^2 = -\left|\underline{q}_\perp\right|^2 \end{cases} \tag{10}$$

In this system the energy differences can be written in the limit $P \to \infty$, i.e., P larger than all other energies,

$$\Delta E = \left(P^2 + M_x^2\right)^{1/2} - (P^2 + M^2)^{1/2} = (M_x^2 - M^2)/2P \tag{11}$$

where M_x defines a typical intermediate state mass coupling to form the proton. Equation (11) just expresses the effect of time dilation on the transition frequencies:

$$\frac{1}{\Delta E} = \left(\frac{2P}{M_x + M}\right) \frac{1}{M_x - M}$$

Thus (9) is satisfied if

$$2M\nu - Q^2 = M_f^2 - M^2 \gg M_x^2 - M^2 \tag{12}$$

Equation (12) is our basic result for applying the impulse approximation or Feynman "parton" model. It defines the deep inelastic region and the criterion for the Bjorken limit[5] — i.e., $P \to \infty$, and

$$\begin{aligned} 2M\nu &\gg M^2 \\ Q^2 &\gg M^2 \\ 2M\nu - Q^2 &\gg M^2 \\ \frac{2M\nu}{Q^2} &= w \text{ finite} \end{aligned} \tag{13}$$

It is here that we may hope to find the scattering to be describable in simple and general terms — and to be computable as well.

The relativistic generalization of (5) for the differential cross section in the rest frame of the target proton is given by

$$\frac{d^2\sigma}{dQ^2 d\nu} = \frac{4\pi\alpha^2}{(Q^2)^2} \left(\frac{\epsilon'}{\epsilon}\right) \left[W_2(q^2, \nu) \cos^2 \theta/2 + 2W_1(q^2, \nu) \sin^2 \theta/2\right] \tag{14}$$

where ϵ and ϵ' are the initial and final energies, θ is the scattering angle of the electron, and $\nu \equiv \epsilon - \epsilon'$. The two structure functions summarizing the hadron

structure in (14) are defined by

$$W_{\mu\nu} = 4\pi^2 \frac{E_p}{M} \sum_m \langle \underline{P} | J_\mu(0) | n \rangle \langle n | J_\nu(0) | \underline{P} \rangle (2\pi)^4 \delta^4(q + P - P_n)$$

$$= -\left(g_{\mu\nu} - \frac{q_\mu q_\nu}{q^2}\right) W_1(q^2, \nu) + \frac{1}{M^2}\left(P_\mu - \frac{P \cdot q}{q^2} q_\mu\right)\left(P_\nu - \frac{P \cdot q}{q^2} q_\nu\right) W_2(q^2, \nu) \tag{15}$$

where $|P\rangle$ is a one-nucleon state with four momentum P_μ, $J_\mu(x)$ is the total hadronic electromagnetic current operator; q_μ is the four momentum of the virtual photon; $q^2 \equiv -Q^2 < 0$ is the square of the virtual photon's mass and $M\nu \equiv P \cdot q$ is the energy transfer to the proton in the laboratory system. An average over the nucleon spin is understood in the definition $W_{\mu\nu}$. The kinematics are illustrated in Fig. 3. It is these two structure functions that we want to focus on. In particular in the high energy limit of (14) so that $\epsilon \longrightarrow \infty$ and $\theta \longrightarrow 0$ the approximate generalization of the sum rule (7) becomes

$$Z \longrightarrow \int_{\nu_{min}}^{\infty} d\nu \, W_2(\nu, q^2) \tag{16}$$

This integral "measures" the charged constituents in the proton.

What does the data tell us? From preliminary measurements[6] such as shown in Fig. 4, which shows small angle data and thus is insensitive to W_1 (unless W_1 is extremely large), it appears that (16) may diverge at least if the present trend of SLAC data continues. Also the absence of a quasi-elastic peak suggests that there may be no well defined "parton" mass—or perhaps the equivalent Fermi distribution is very broad. However, the graph reveals (for νW_2) a very important general feature anticipated by Bjorken[5] on the basis of formal field theoretic arguments and that is that the structure functions $W_1(q^2, \nu)$ and $\nu W_2(q^2, \nu)$ are

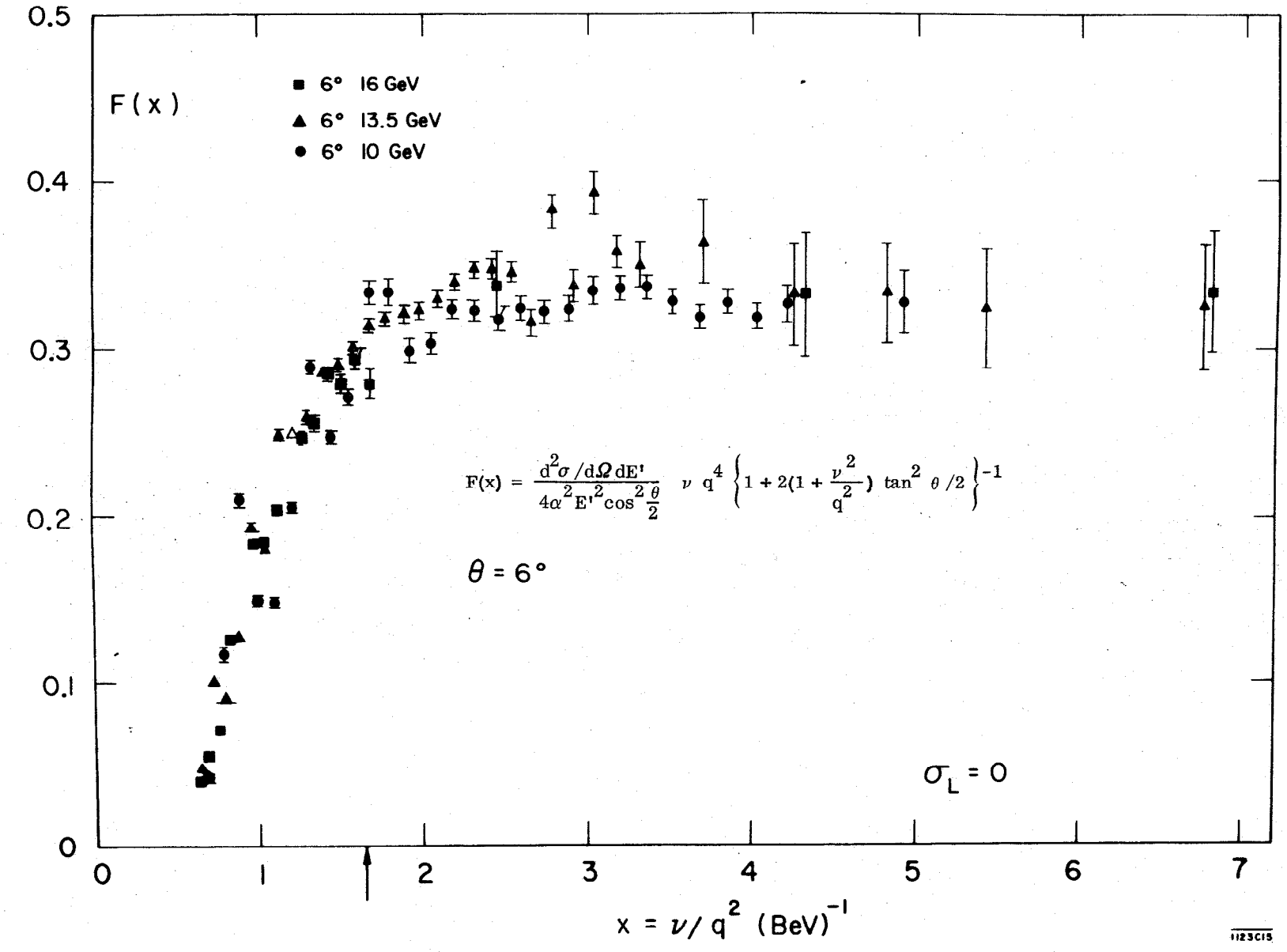
F(x)
■ 6° 16 GeV
▲ 6° 13.5 GeV
● 6° 10 GeV
$F(x) = \frac{d^2\sigma/d\Omega dE'}{4\alpha^2 E'^2 \cos^2\frac{\theta}{2}} \; \nu \; q^4 \left\{1 + 2(1 + \frac{\nu^2}{q^2}) \tan^2 \theta/2\right\}^{-1}$
$\theta = 6°$
$\sigma_L = 0$
0.5
0.4
0.3
0.2
0.1
0
0
1
2
3
4
5
6
7
$x = \nu/q^2$ (BeV)$^{-1}$
1123C15

FIG. 4

functions of $w = 2M\nu/Q^2$ alone, i.e.,

$$MW_1(q^2, \nu) = F_1(w)$$

$$\nu W_2(q^2, \nu) = F_2(w)$$

$$\text{for } Q^2, 2M\nu \gg M^2 \tag{17}$$

This behavior can also be derived by qualitative physical arguments as shown by Feynman[4] on the basis of his parton model. In brief we may view the protons as composed of "free" or "long lived" partons according to the discussion leading up to (13) so long as we are in the Bjorken limit and can apply an impulse approximation. In this limit with $\underline{P} \longrightarrow \infty$ each parton is moving approximately along $\underline{P}$ since its transverse momentum is negligible in comparison with the longitudinal momentum $\eta\underline{P}$; $0 < \eta < 1$. The distribution in η represents the longitudinal momentum distribution of the partons or elementary consitituents of the proton in an infinite momentum ($P \longrightarrow \infty$) frame. According to criterion (12) these "free" partons interact instantaneously with the electromagnetic current and if they are point particles this interaction is proportional to their charge or static moments (if any) and contains no form factor dependence $f(q^2)$. To leading order they acquire only a transverse momentum $q_\perp \approx \sqrt{Q^2}$ by (10) and remain on their mass shells with the same mass, i.e.,

$$(\eta P + q)^2 = M^2_{\text{Parton}} = M^2_{\text{Parton}} - Q^2 + 2\eta M\nu \tag{18}$$

This tells us that $Q^2 = \eta(2M\nu)$ or the structure depends on the longitudinal momentum distribution viewed in an infinite momentum frame, $\eta = 1/w$, alone. This distribution is what the measurements tell us as a function of w.

Now let us ask two questions. First: is there any sense to the parton model? Second: why does the behavior of the structure functions experimentally look so different from the picture suggested by the analogy with nuclear scattering?

In these lectures I want to derive a parton model from canonical field theory not only for scattering but also for pair annihilation in the deep inelastic region.[7] I derive this model not because I particularly like or want to preserve field theory, but because it is not enough to explain the scaling low; it is necessary to have also some predictive power, in particular for the crossed reaction:

$$e^- + e^+ \longrightarrow p + \text{"anything"}$$

and field theory, with its crossing properties, can give some clue about this. In fact we can derive a parton model for all the processes

$$e^- + p \longrightarrow e^- + \text{"anything"}$$

$$e^+ + e^- \longrightarrow p + \text{"anything"}$$

$$\nu(\bar{\nu}) + p \longrightarrow e^-(e^+) + \text{"anything"}$$

as well as for other hadron charges and SU_3 quantum members. It follows from this result that all the structure functions depend only on w as conjectured by Bjorken for the deep inelastic scattering. To accomplish this derivation it is necessary to introduce a transverse momentum cutoff so that there exists an asymptotic region in which q^2 and $M\nu$ can be made larger than the transverse momenta of all the partons that are involved. Upon crossing to the e^+e^- annihilation channel, an operation we can perform using our field theory basis, and deriving a parton model for this process we arrive at the important result that the deep inelastic annihilation cross section to a hadron plus "anything" is very large, varying with colliding e^-e^+ beam energy at fixed w in the same way as do point lepton cross sections. This result has important general implications for colliding ring experiments as well as for the ratios of annihilation to scattering cross sections and of neutrino to electron-inelastic scattering cross sections.

Before developing a formalism for deriving the parton model we can answer the second of the above questions of where the analogy with the nuclear scattering

goes wrong. Underlying the difference between Z and the apparently diverging right-hand side of (16) is the presence of an additional physical interaction mechanism present in high energy strong interaction processes but absent from the atomic and nuclear realm and that is diffraction scattering. At high energies above meson production thresholds many new channels open up leading to constant total cross sections for hadrons in the high energy limits as the incident nucleons, pions, or photons are absorbed on a black or very dark grey disk. Indeed the structure functions can be directly related to cross sections for absorption of virtual photons of mass $-Q^2$. The connection of the lower half of Fig. 3 or of the amplitude (15) with a cross section is a matter of algebra and consistent normalizations.

Following Hand's[8] definitions there results

$$W_1 = \frac{1}{4\pi^2\alpha}(\nu - Q^2/2M)\sigma_t \tag{19a}$$

$$\nu W_2 = \frac{1}{4\pi^2\alpha}(1 - Q^2/2M\nu)Q^2\left(\frac{\sigma_t + \sigma_\ell}{1+Q^2/\nu^2}\right) \tag{19b}$$

where by $\sigma_{t,\ell}(Q^2,\nu)$ is meant the total cross section for a transversely or longitudinally polarized photon of mass $-Q^2$ to form a state of the same total mass (i.e., $s = (q + P)^2$) as a real photon of the same laboratory frequency. Evidently from (19b) if the total cross sections approach constants for virtual photons, as they do for hadrons on protons, νW_2 is expected also to approach an energy independent constant for fixed large Q^2 as $\nu \longrightarrow \infty$: $\nu W_2 \longrightarrow \frac{1}{4\pi^2\alpha} Q^2(\sigma_t + \sigma_\ell)$. This suggests that the data should continue its present trend leading the right-hand side of (16) to diverge logarithmically. It is also apparent from (19b) that the Bjorken prediction as well as the observation that $\nu W_2 = F_2(w)$ as in (17) requires

$$\sigma_t + \sigma_\ell \propto \frac{1}{Q^2} f(w)$$

and more particularly if we accept the present trend as well as the simple Regge theory notion of constant total cross sections at high energy

$$\sigma_t + \sigma_\ell \propto \frac{1}{Q^2} \quad \text{for large } Q^2 \text{ as } \nu \longrightarrow \infty \tag{20}$$

This contrasts a $\frac{1}{Q^8}$ falloff for elastic or resonance scattering as in (2). The natural emergence of this type of behavior has been discussed by Abarbanel, Goldberger, and Treiman[9] from the study of ladder graphs contributing to forward virtual Compton scattering — or to the total cross section by the optical theorem. From the same conjectured behavior (20) in contrast to the more rapid falloff of resonance excitations Harari[10] has suggested that the diffraction mechanism (or Pomeron exchange) responsible for constant total cross sections dominates at all energies for $Q^2 \longrightarrow \infty$ and has derived and discussed implications of this suggestion. This behavior and the underlying diffraction mechanism are seen as the reasons for the inadequacy of the analogy in (16). We turn then to a more formal theoretical approach — and in particular one which will provide a basis for crossing to the colliding beam region of interest for deep inelastic $e^- - e^+$ annihilation.

The derivation of the parton model for inelastic scattering will be carried out in the infinite momentum center-of-mass frame of the electron and proton (10) with the nucleon momentum P along the 3 axis. Let us use good old-fashioned perturbation theory (OFPT) which in the $P \longrightarrow \infty$ frame enjoys some great calculation simplifications. We undress the current operator and go into the interaction picture with the familiar U matrix transformation

$$J_\mu(x) = U^{-1}(t)\, j_\mu(x)\, U(t), \quad U(t) = \left(e^{-i\int_{-\infty}^{t} H_I(\tau)\, d\tau} \right)_+ \tag{21}$$

where $J_\mu(x)$ is the fully interacting electromagnetic current and $j_\mu(x)$ the corresponding free or bare current. Equation (15) can now be rewritten as

$$W_{\mu\nu} = 4\pi^2 \frac{E_p}{M} \sum_n \langle UP | j_\mu(0)\, U(0) | n \rangle \langle n | U^{-1}(0)\, j_\nu(0) | UP \rangle (2\pi)^4 \delta^4(q + P - P_n) \tag{22}$$

where

$$|UP\rangle = U(0)|P\rangle .$$

A basic ingredient in the derivation of the parton model from canonical field theory is the existence of an asymptotic region in which Q^2 can be made greater than the transverse momenta of all particles involved, i.e., of the pions and nucleons emitted into real final states and that also are the (virtual) constituents of $|UP\rangle$. We must assume the existence of such a region in our formal theoretical manipulations. Such an assumption is in agreement with present high energy data that strongly indicate that transverse momenta of the final particles are indeed very limited in magnitude. (Further discussions of this point and its basis are reserved for the question session.)

Let us recall that in the infinite momentum frame, because of the time dilation factor, one can construct on a physical basis, as shown by Feynman, a "free constituent picture." Our present goal is to translate this into a formal derivation, and then to derive the "impulse approximation" and a "parton" model from field theory, for processes with large energy and momentum transfers.

Now OFPT makes unitarity more evident than relativistic Feynman rules. On the other hand, the Feynman amplitudes are manifestly covariant and the OFPT ones are not. The main point is however the following: in OFPT one indeed has at each vertex conservation of momentum but not of energy; all internal particles are on their mass shells. The relativistic time dilation factor however, in the $P \to \infty$ frame, implies under certain circumstances also the approximate conservation of energy, so that we can recapture covariance.

So we work with OFPT in the $P \to \infty$ frame, starting with the undressing transformation (21). These things are nicely discussed, for the spinless case, in Weinberg's[11] paper; the realistic case is however much more delicate.

To see what happens to our basic object $W_{\mu\nu}$ in this frame and in the Bjorken limit we write from (22)

$$W_{\mu\nu} = 4\pi^2 \frac{E_p}{M} \sum_n (2\pi)^4 \langle UP|j_\mu(0)|Un\rangle\langle Un|j_\nu(0)|UP\rangle \delta^4(q + P - P_n)$$

$$= 4\pi^2 \frac{E_p}{M} \sum_n \int d^4x \; e^{iq\cdot x} e^{i(P - P_n)\cdot x} \langle UP|j_\mu(0)|Un\rangle\langle Un|j_\nu(0)|UP\rangle \qquad (22')$$

Now $P^0 = E_p$ and $(P_n)^0 = E_n$ are the energies of the exact eigenstates $P\rangle$ and $n\rangle$ respectively. However the states $UP\rangle$ and $Un\rangle$ are not energy eigenstates. Let us denote by E_{up} and E_{un} the energies of the "unperturbed" individual components contributing in their perturbation expansion — i.e., the energies of the individual states contributing to the series developed from (21):

$$|UP\rangle = \sqrt{Z_2}\left\{|P\rangle + \sum_m{}' \frac{m\rangle\langle m|H_I|P\rangle}{E_p - E_m} + \sum_{m,r}{}' \frac{m\rangle\langle m|H_I|r\rangle\langle r|H_I|P\rangle}{(E_p - E_m)(E_p - E_r)} + \cdots\right\}$$

where $\sum'$ indicates the summation over all intermediate states <u>except</u> $|P\rangle$ and Z_2 is the proton's wave function renormalization constant. <u>If</u> $E_p - E_{up} \longrightarrow 0$ and $E_n - E_{un} \longrightarrow 0$ in our asymptotic limit then the four momentum operator P^μ_{op} commutes with U(0), which automatically conserves momentum, and the exponential can be changed into a displacement operator. At this point one has the closure sum: $\sum |n\rangle\langle n| = 1$ so that:

$$\lim_{\substack{P\longrightarrow\infty \\ q^2,\, M\nu\longrightarrow\infty}} W_{\mu\nu} = \frac{4\pi^2}{M} E_p \int d^4x \; e^{iq\cdot x} \langle UP|j_\mu(x)\, j(0)|UP\rangle \qquad (23)$$

This equation can be regarded as the field-theoretical derivation of the parton model: i.e., the proton is an infinite sum: proton, proton + pion, proton + nucleon + antinucleon, etc. (no defined set of numbers; this is the full perturbation expansion) and the current operator is the free (bare) one. It is in this way that we come to the impulse approximation. Once we have derived a result like this, we can proceed to deduce scaling laws, etc.

Notice that the crux of this derivation lies in the replacement of E_p by E_{up} and E_n by E_{un}, which we now will discuss in further detail. The assumption has been made that the particles emitted or absorbed at any strong vertex have only finite transverse momenta. Then both $U|P\rangle$ and $U|n\rangle$ can be treated as eigenstates of the Hamiltonian with eigenvalues E_p and E_n, respectively. To show this let E_{up} symbolically denote the energy of one of the multi-pion + nucleon states in the perturbation expansion of $|UP\rangle$. In the infinite momentum frame, $E_p - E_{up}$ is of the order of $1/P$ multiplied by the sum of squares of some characteristic transverse momentum and some characteristic mass. For example let $|UP\rangle$ denote a state of one nucleon with momentum $\eta\underline{P} + \underline{k}_\perp$ plus one pion with $(1-\eta)\underline{P} - \underline{k}_\perp$ in accord with momentum conservation; take $\underline{k}_\perp \cdot \underline{P} = 0$. We also take the fraction of momentum carried by the nucleon and pion lines respectively, η and $(1-\eta)$ to be positive along the $\underline{P}$ direction. The kinematics are shown in Fig. 5. We find then, for $P \longrightarrow \infty$

$$E_p - E_{up} = \left(\underline{P} + \frac{M^2}{2\underline{P}}\right) - \left(\eta\underline{P} + \frac{k_\perp^2 + M^2}{2\eta P}\right) - \left((1-\eta)\underline{P} + \frac{k_\perp^2 + \mu^2}{2(1-\eta)\underline{P}}\right)$$

$$= -\frac{1}{2P}\left[\frac{k_\perp^2}{\eta(1-\eta)} + \frac{M^2(1-\eta)}{\eta} + \frac{\mu^2}{1-\eta}\right] \qquad (24)$$

This difference in (24) will generally be negligible in comparison with the photon energy q^o as given in (10) and therefore can be neglected in the energy delta function $\delta(q_0 + E_p - E_n)$ appearing in (22) provided we work in the Bjorken limit, $2M\nu - Q^2 \gg M^2$ and we restrict $k_{\perp\,\max}^2 \ll Q^2$. This argument fails for the regions of momenta $\eta < 0$ or >1 which lead to $E_{up} - E_p \sim P$ corresponding to particles moving anti-parallel as well as parallel to P. However by analyses such as described by Weinberg[11] we establish that for these regions of η the energy denominators introduced by the time integrals appearing in the expansion of the

time-ordered products of U(0),

$$U(0) = \left(e^{-i\int_{-\infty}^{0} H_I(t)dt} \right)_+$$

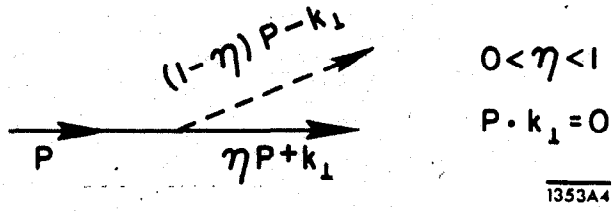

FIG. 5

lead to contributions to $W_{\mu\nu}$ reduced by factors of 1/P. This analysis will be spelled out in detail in a forthcoming paper,[7] but can be sketched here adequately. In particular we must work only with the good components of the current, i.e., J_μ for = 0 or 3 along the direction of P. Otherwise the diagrams with particles moving with $\eta < 0$ or >1 cannot be excluded because the extra powers of P in the denominator can be compensated by similar factors in the numerator from matrix elements of the bad components of the current, that is J_1 and J_2 in the $P_3 \to \infty$ frame. However we can compute the contributions of the good components only — i.e., W_{00} and W_{33} — and by covariance construct the whole tensor.

Let us sketch the proof of the above statements for the case $\eta < 0$ and $\eta > 1$. The old-fashioned perturbation formula reads:

$$U|a\rangle = \sqrt{Z}\left\{|a\rangle + \sum_{n_1}{}' |n_1\rangle \frac{\langle n_1|H_I|a\rangle}{E_a - E_{n_1}} + \sum_{n_1, n_2}{}' \frac{|n_2\rangle\langle n_2|H_I|n_1\rangle\langle n_1|H_I|a\rangle}{(E_a - E_{n_1})(E_a - E_{n_2})} + \ldots \right\}$$

where a is some unperturbed state, and Z a renormalization constant. This formula shows that in computing the magnitude of each contribution there are equal numbers of numerator matrix elements and energy denominators to be considered. In the infinite momentum frame, as illustrated in (24), the energy denominators can be

either:

$$E_a - E_{n_1} \sim 1/P \text{ (and we call them good) or}$$

$$E_a - E_{n_1} \sim P \text{ (and we call them bad).}$$

However the bad denominators can be balanced, but for each bad denominator giving an added factor $\frac{1}{P^2}$ there must be two compensating "bad" numerators. As an example, let us consider the usual pseudoscalar coupling between pions and nucleons $\mathscr{L}_I = g\bar{\psi}\gamma_5\psi\phi$.

It is not difficult to show that in the $P \longrightarrow \infty$ frame, vertices corresponding to this coupling are of the order 1 (small vertices) in the case of (anti-) nucleons moving along the same direction through the interaction, and of order P (big vertices) in the case of (anti-) nucleons moving along opposite directions; this is left as an exercise. This property defines a "bad" current, such as 1, γ_5, or the transverse current components γ_1 and γ_2; "good" currents such as γ_0 and γ_3 in contrast have just the opposite behavior.

The good currents are penalized rather than enhanced by a factor of 1/P when they turn a line moving along $\vec{P}$ into one moving against it as $P \longrightarrow \infty$. It is this simple observation plus the need to balance each bad denominator with two compensating numerators that allows us to proceed. In Fig. 6 we illustrate a series of graphs, the ones labeled "yes" meaning they survive to leading order as $P \longrightarrow \infty$, and the ones labeled "no" meaning they are reduced by one or more powers of P in this limit. Note that we do simple power counting assuming that all expressions are convergent which is one of the reasons we have to supply a transverse momentum cutoff.

In these graphs time runs to the right and arrows to the right mean momenta along $\underline{P}$.

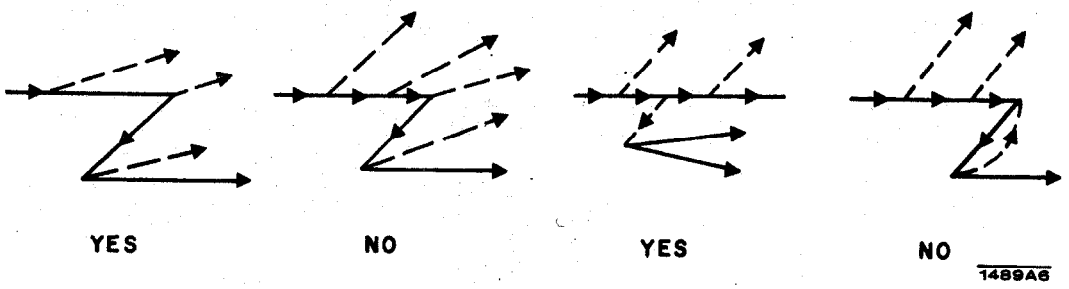

FIG. 6

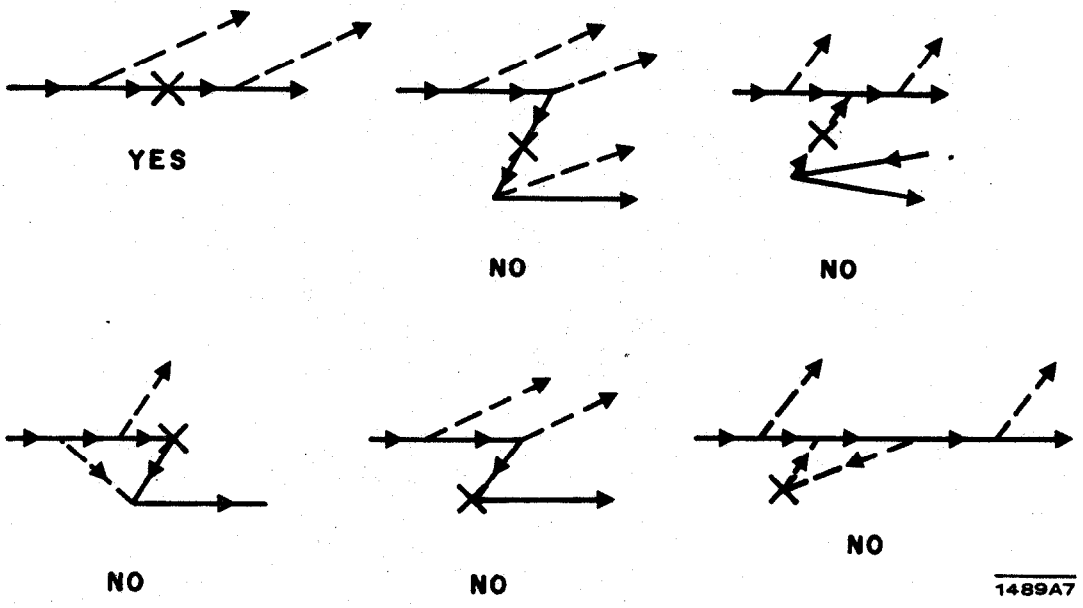

FIG. 7

Examples of graphs with a vertex for a "good" external current denoted by an x are shown in Fig. 7 along with the corresponding "yes" or "no" for leading contributions as $P \longrightarrow \infty$. Proceeding in this graphical manner we can arrive at the following general statement: any final particle belonging to the state $|UP\rangle$, i.e., one existing just before the moment when j_μ acts in (22') or (23) must go to the right along $\vec{P}$. Otherwise j_μ cannot change its direction, since $q_{long} \simeq 0$ even if it does land on it, or because j_μ does not interact with this particular line.

Therefore it will enter into the state $|Un\rangle$ still moving to the left and hence there will appear in its contribution to $W_{\mu\nu}$ at least two bad denominators but only two big vertices at most, which cannot compensate them. Thus whatever so called "Z graphs" may appear intermediately as illustrated in Fig. 6, all lines eventually emerging into $|UP\rangle$ move to the right satisfying the criterion indicated above for replacing E_{up} by E_p in our problem. Since j_0 and j_3 introduce negligible longitudinal momentum by (10) all lines also will continue to move to the right in $|Un\rangle$. Finally no lines can move to the left against $\vec{P}$ in the final state $|U\rangle$ in the infinite momentum frame as a result of energy conservation and so our claim is established.

There is a second class of simplifications in the Bjorken limit if we now take into account the existence of a bound on $k_\perp$, which allows us to count powers of $1/Q^2$ retaining again only the leading contributions.

To make these simplifications apparent we consider the time-ordered sequence of events in the old-fashioned perturbation theory description of a scattering process as represented by the matrix element $\langle UP|j_\mu(0)U|n\rangle$. Before the bare current $j_\mu(0)$ operates, $|UP\rangle$ describes emission and reabsorption of pions and nucleon-antinucleon pairs. The bare electromagnetic current scatters one of the charged constituents in $|UP\rangle$ and imparts to it a very large transverse momentum $\underset{\sim}{q}_\perp \approx \sqrt{Q^2}$. The unscattered constituents in $|UP\rangle$ keep moving and emit and reabsorb pions and nucleon-antinucleon pairs. They form a group of particles moving very close to each other along the direction $\underset{\sim}{P}$ as large transverse momenta are suppressed by the cutoff vertices. The scattered charged constituent also emits and reabsorbs pions and nucleon-antinucleon pairs. Analogously these form a second group of particles moving close to each other but along a direction which deviates in transverse momentum by $\underset{\sim}{q}_\perp$ from the first group. These two groups of particles,

denoted by (A) and (B), are illustrated in Fig. 8. As $\underset{\sim}{q}_\perp \longrightarrow \infty$ the cutoff strong vertices prevent any particle emitted by group (A) from being absorbed by group (B) and vice versa. Consequently, there is no interaction between the two well-separated groups of particles. It is then obvious that diagrams contributing to $W_{\mu\nu}$ and corresponding to electromagnetic vertex corrections (Fig. 9) or more complicated diagrams describing interactions between the two groups of particles (Fig. 10) vanish in the limit $\underset{\sim}{q}_\perp \longrightarrow \infty$. It is equally obvious that coherent interference between the two matrix elements $\langle UP|j_\mu(0)U|n\rangle$ and $\langle n|U^{-1}j_\nu(0)|UP\rangle$ in (22) is impossible unless they both produce the identical sets of well-separated particle groups (A), (B) and (A'), (B'). As a result diagrams of the type given in Fig. 11 vanish as $\underset{\sim}{q}_\perp \longrightarrow \infty$. In Figs. 9. 10, and 11 we are representing squares of matrix elements appearing in $W_{\mu\nu}$ and the dashed verticle line denotes a real physical final state formed from the initial proton.

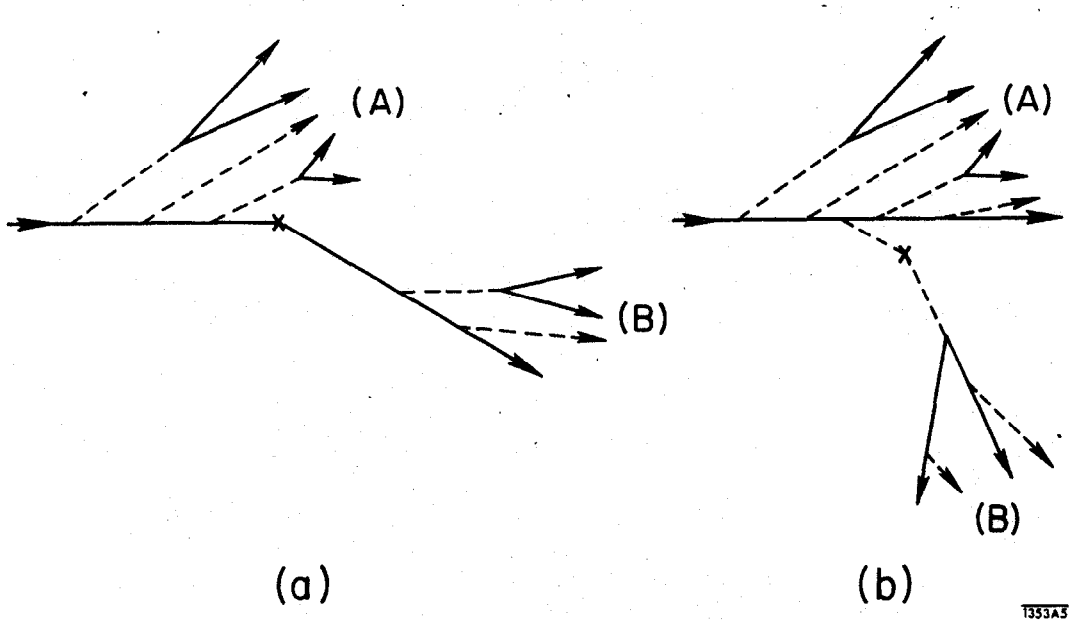

FIG. 8

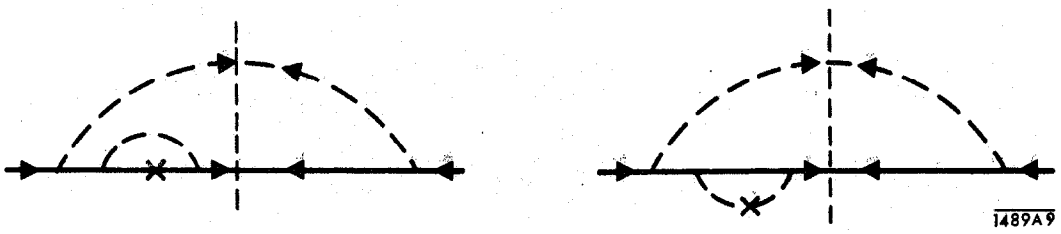

FIG. 9

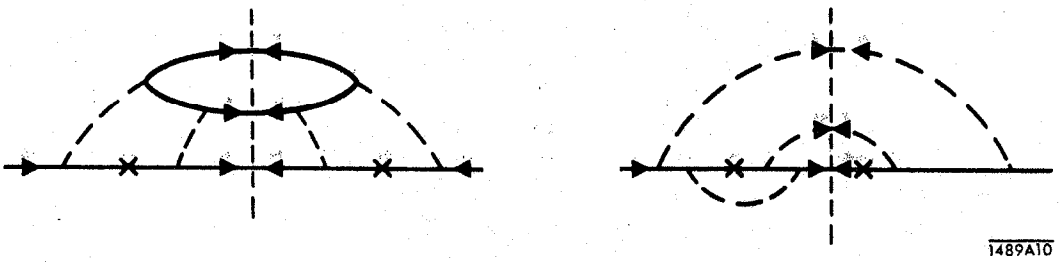

FIG. 10

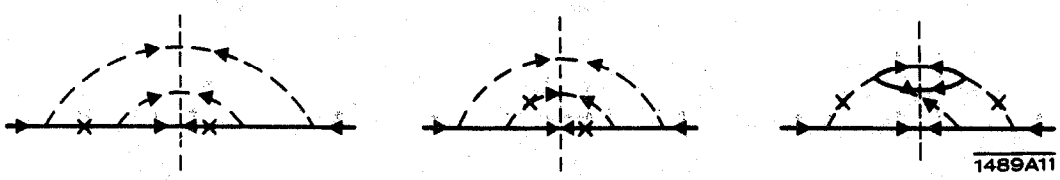

FIG. 11

In the lab frame this process looks as follows: The constituents of the proton in group (B) of Fig. 8 emerge with very high momenta along q while the rest in group (A) are left behind. The invariant mass of each of the two groups is small since the transverse momenta of the constituents do not spread far away from each other. The energy differences between $|P\rangle$ and $|UP\rangle$, $|n$ and $|U(0)|n\rangle$ are therefore negligible in the limit of large Q^2 and $M\nu$ as we argued in (24).

Since there is no interference between the two groups of particles, the U operator acts separately and independently on each of the two groups (A) and (B)

in Fig. 8. Our derived result simply states the fact that the total probability that anything happens among the particles in each of the two groups (A) and (B) is unity because of unitarity of U. An example of this result is illustrated by the graphs in Fig. 12. It can also be seen by inserting a complete set of states between the current operators in (23) and neglecting the difference $E_p - E_{up}$ as discussed above in displacing the current to the origin. This operation gives (22) or (22') with $U|n\rangle \longrightarrow |n\rangle$.

The result of Eq. (23) established the "parton model" by allowing us to work with free point currents and the superposition of essentially free (i.e., long-lived) constituents in describing the proton's ground state in the infinite momentum frame and in the Bjorken limit.

In particular the form of (23) assures us of universal behavior. If the bare current $j_\mu(x)$ lands on a constituent in $|UP\rangle$ with momentum P_a, $P_a^2 \simeq M_a^2$ it scatters it on to the mass shell with $P_a + q$ and $(P_a + q)^2 \equiv M_a^2$. By simple

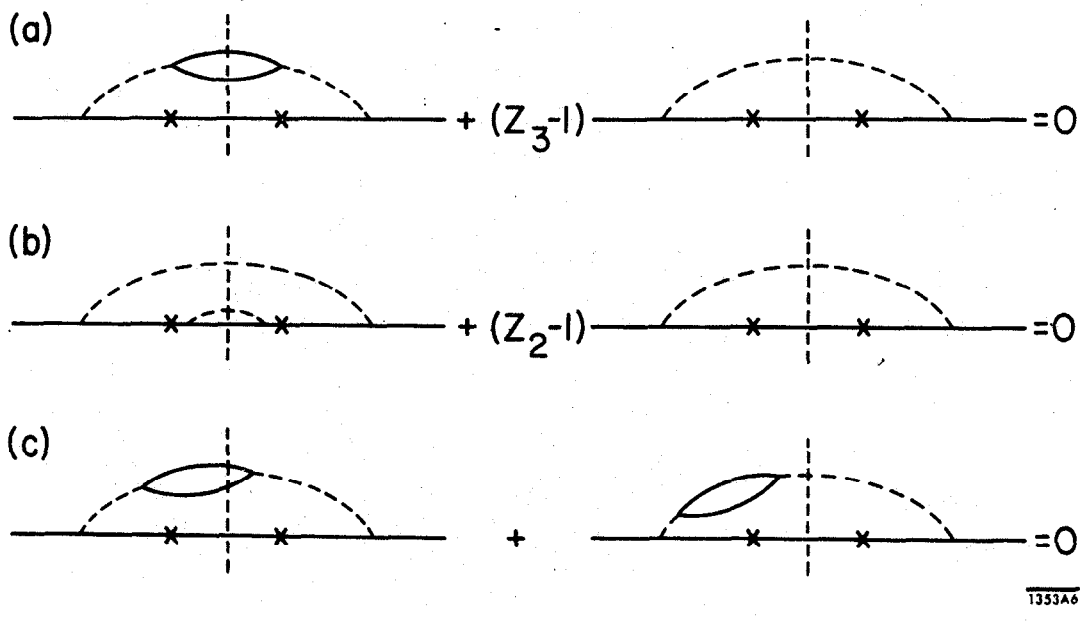

FIG. 12

integration of (23) this mass shell constraint emerges as a delta function

$$\delta\left(2P_n \cdot q - Q^2\right) \cong \delta(2\eta M\nu - Q^2) = \frac{1}{2M\nu}\,\delta\left(\eta - \frac{1}{w}\right) \tag{25}$$

where we have used (10) and η is the fraction of longitudinal momentum borne by the constituent on which the bare current lands. Equation (23) leads to a universal behavior of W_1 and νW_2 as functions of w as predicted by Bjorken[5] and shows that the observed w dependence reflects the longitudinal momentum distribution of the constituents in the infinite momentum frame.

The detailed calculations of the functional forms for W_1 and νW_2 were worked out in Ref. 7 for large $w \gg 1$.

It remains for us only to verify that the result presented by (23) is actually finite and nonvanishing — i.e., to show that we have actually retained the leading contribution in the Bjorken limit. We do this by the following construction. We expand $|UP\rangle$ in terms of a complete set of multiparticle states

$$|UP\rangle = \sum_n a_n |n\rangle\,; \quad \sum_n |a_n|^2 = 1 \tag{26}$$

Introducing this into (23) we use the following relation to identify W_2, the coefficient of $P_\mu P_\nu$

$$\int (dx) e^{iqx} \langle P_{n,i} | j_\mu(x)\, j_\nu(0) | P_{n,i} \rangle = \frac{1}{4\pi^2}\,\frac{1}{E_{n,i}}\, 2P_{n,\mu}\, P_{n,\nu}\, \delta(Q^2 - 2M\nu\,\eta_{n,i}) + \cdots$$

$$= \frac{P_\mu P_\nu}{4\pi^2 P}\,\frac{1}{M\nu w}\,\delta\left(\eta_{n,i} - \frac{1}{w}\right) + \cdots \tag{27}$$

$P_{n,i}$ is the four momentum of the charged constituent on which the current lands, and $\eta_{n,i}$ has the same meaning as in (25); the dots indicate the additional contributions to the structure function W_1. The charged constituent can be a $\pi^{\pm}$, P or $\overline{P}$. For the nucleon current the above equation follows from the use of projection matrices $(M + \gamma P_n)$ and $(M + \gamma(P_n + q))$ before and after the current acts. Then

symbolically we have

$$\nu W_2 = \frac{1}{w} \sum_n |a_n|^2 \langle n | \sum_i \delta\left(\eta_{n,i} - \frac{1}{w}\right) \lambda_{n,i}^2 | n \rangle$$

where $\lambda_{n,i}$ is the charge of the i^{th} constituent in state $|n\rangle$. This relation gives a sum rule

$$\int_1^\infty \frac{dw}{w} (\nu W_2) = \sum_n \left(\sum_i \lambda_{n,i}^2\right) |a_n|^2 = \sum_n |a_n|^2 n_c$$

where n_c is the number of charged constituents in state $|n\rangle$. We have here implicitly assumed that the constituents are all integrally charged as is the case in our model of pions and nucleons. Thus the weighted integral of νW_2 over w may be interpreted as the mean number of charged physical constituents in the transformed proton state $UP\rangle$. It follows from $n_c \geq 1$ and the normalization condition of a_n's that

$$\int_1^\infty \frac{dw}{w} (\nu W_2) \geq 1 \tag{28}$$

This inequality is trivial to satisfy if the SLAC data continues its present trend with νW_2 apparently approaching a constant for large w.

The area under the integral as measured so far up to $w_{max} \sim 20$ is roughly 0.7. The ratio of W_1 to νW_2 is determined in (27) by the fact that the fraction of longitudinal momentum carried by the charged constituent on which the current lands is fixed at $\eta = 1/w$ by the δ-function. It is an easy calculation to show that for $j_\mu(x)$ representing a pion or a spinless boson $W_1 = 0$ whereas for $j_\mu(x)$ a nucleon current $\frac{W_1}{\nu W_2} = \frac{w}{2M}$. Their ratio as measured from the angular distribution in (14) will reveal the spin nature of the dominant current interaction in the Bjorken limit.

Now we will consider the process:

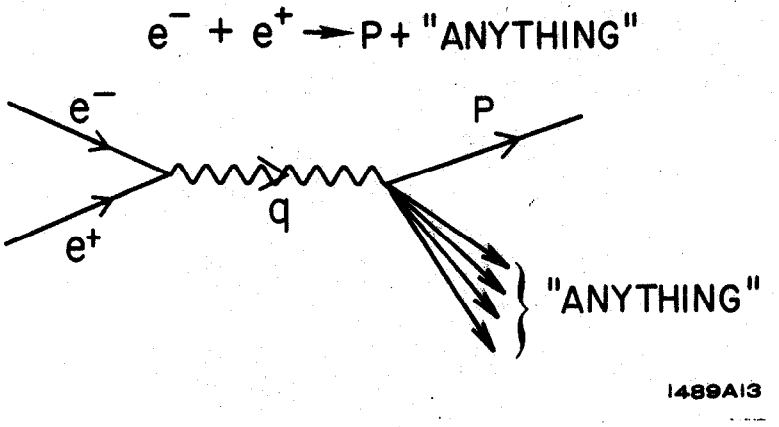

FIG. 13

which can be related by crossing to the deep inelastic scattering examined up to now.

In this case we have $q^2 > 0$ (time-like photon) and $q \cdot P = M\nu$ is the energy transfer to all the hadrons in the rest system of the detected one. Our basic object will be, as before, the quantity

$$\overline{W}_{\mu\nu} = 4\pi^2 \frac{E_p}{M} \sum_n (2\pi)^4 \delta(q - P - P_n) \langle 0 | J_\mu(0) | Pn \rangle \langle nP | J_\nu(0) | 0 \rangle$$

$$= -\left(g_{\mu\nu} - \frac{q_\mu q_\nu}{q^2}\right) \overline{W}_1(q^2, \nu) + \frac{1}{M^2}\left(P_\mu - \frac{P \cdot q\, q_\mu}{q^2}\right)\left(P_\nu - \frac{P \cdot q}{q^2} q_\nu\right) \overline{W}_2(q^2, \nu) \quad (29)$$

Now, exactly as before, the question arises: have these functions a scaling behavior, etc... ?

First of all, let us examine the kinematical region for the annihilation process. Now we want to detect a proton in the final state, so that we must have $q^2 > 4M^2$; moreover, ν_{min} will be the energy transfer to the proton detected at rest: i.e., since $M\nu = P \cdot q$, $\nu_{min} = \sqrt{q^2}$ (notice that, in the colliding beam system, $q = (q_0, 0)$). ν_{max} will correspond to the elastic annihilation process $e^+ + e^- \rightarrow \overline{p} + p$,

so that the kinematical region in the $(q^2,\ 2M\nu)$ plane is bounded by the $\nu = \sqrt{q^2}$ parabola and the $q^2 = 2M\nu$ straight line (see figure below)

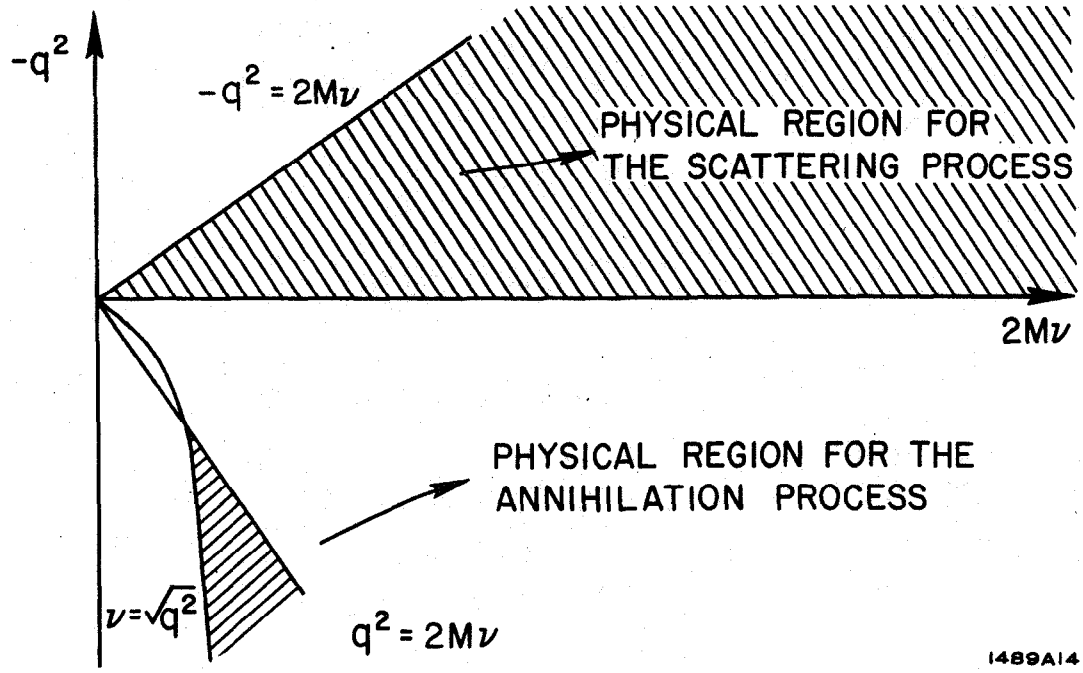

FIG. 14

In the colliding beam frame the cross section reads:

$$\frac{d^2\sigma}{dEd(\cos\theta)} = \frac{4\pi^2\alpha^2}{(q^2)^2}\,\frac{M^2\nu}{\sqrt{q^2}}\sqrt{1-\frac{q^2}{\nu^2}}\left[2\overline{W}_1(q^2,\nu)+\frac{2M\nu}{q^2}\left(1-\frac{q^2}{\nu^2}\right)\frac{\nu\overline{W}_2(q^2,\nu)}{2M}\sin^2\theta\right] \tag{30}$$

where E is the energy of the detected proton and θ is the angle of the proton momentum $\underset{\sim}{P}$ with respect to the axis defined by the incident colliding e^- and e^+ beams.

By straightforward application of the reduction formalism to the proton P in the states in (15) and (29) it readily shown that $\overline{W}_{\mu\nu}$ and $W_{\mu\nu}$ are related by the substitution law

$$\overline{W}_{\mu\nu}(q,\ P) = -W_{\mu\nu}(q,\ -P)$$

$$\overline{W}_1(q^2,\nu) = -\ W_1(q^2,\ -\nu),\quad \nu\overline{W}_2(q^2,\ \nu) = (-\nu)W_2(q^2,\ -\nu) \tag{31}$$

Let us write for space-like q^2

$$MW_1(q^2, \nu) = F_1(w, s) \quad \nu W_2(q^2, \nu) = F_2(w, s)$$

where $w \equiv \frac{2M\nu}{-q^2} > 1$ and $s \equiv (q + P)^2 = 2M\nu - Q^2 + M^2 > M^2$. In the Bjorken limit ($\lim_{bj}$) we have

$$\lim_{bj} MW_1(q^2, \nu) = F_1(w) = \lim_{s\to\infty} F_1(w, s) \qquad (w > 1)$$

$$\lim_{bj} \nu W_2(q^2, \nu) = F_2(w) = \lim_{s\to\infty} F_2(w, s)$$

The substitution law (31) gives for time-like q^2

$$M\overline{W}_1(q^2, \nu) = -F_1(w, s), \quad \nu\overline{W}_2(q^2, \nu) = F_2(w, s)$$

where $0 < w = \frac{2M\nu}{q^2} < 1$ and $s = (q - P)^2 = q^2 - 2M\nu + M^2 > M^2$. If we can show that the Bjorken limit exists for time-like q^2, we expect to find in general

$$\lim_{bj}(-)\, M\overline{W}_1(q^2, \nu) = \overline{F}_1(w) = \lim_{s\to\infty} F_1(w, s) = F_1(w)$$

$$\lim_{bj} \nu\overline{W}_2(q^2, \nu) = \overline{F}_2(w) = \lim_{s\to\infty} F_2(w, s) = F_2(w) \qquad (32)$$

namely, $\overline{F}_1(w)$ and $\overline{F}_2(w)$ are the continuations of the corresponding functions $F_1(w)$ and $F_2(w)$ from $w > 1$ to $w < 1$. Relations (32) will be true, for example, if the Bjorken limits are approached algebraically so the sign change in $w-1$ between $w > 1$ for scattering and $0 < w < 1$ for pair annihilation will not have any pathological effect. We shall now demonstrate, using as an example the model of charge symmetric theory of pseudoscalar pions and nucleons with γ_5 coupling and with a transverse momentum cutoff, that firstly, the Bjorken limits of $\overline{W}_1$ and $\nu\overline{W}_2$ exist, and secondly, the relations (32) are indeed satisfied.

A convenient infinite momentum frame for this analysis is one in which

$$q^\mu = \left(q_3 + \frac{q^2}{2q_3},\ 0,\ 0,\ q_3\right) \quad P^\mu = \left(P + \frac{M^2}{2P},\ 0,\ 0,\ P\right) \qquad (33)$$

For large $q^2 \gg M^2$ we have, since $q \cdot P \doteq M\nu$,

$$q_3 = \frac{q^2}{2M\nu} P = \frac{1}{w} P \tag{34}$$

In analogy to our discussion of (22) we undress the current by substituting (21) into (29). There is an immediate simplification if we restrict ourselves to studying the good components of J_μ ($\mu = 0$ or 3). For these components we can ignore the U(0)'s acting on the vacuum, and obtain from (29)

$$\overline{W}_{\mu\nu} = 4\pi^2 \frac{E_p}{M} \sum_n \langle 0 | j_\mu(0) U(0) | Pn \rangle \langle nP | U^{-1}(0) j_\nu(0) | 0 \rangle (2\pi)^4 \delta^4(q - P - P_n) \tag{35}$$

The reason for this simplification is similar to that discussed in connection with the inelastic scattering. If U(0) operates on the vacuum state it must produce a baryon pair plus meson with zero total momentum so that at least one particle will move toward the left and another toward the right along $\underset{\sim}{q}$ or $\underset{\sim}{P}$.

Thus there will appear one or more large energy denominators of order $\sim P$ instead of $\sim 1/P$. However when working with the good components of the current — i.e., J_0 or J_3 along $\underset{\sim}{P}$ an inadequate number of compensating factors of P are introduced into the numerator by the vertices and so such terms can be neglected in the infinite momentum limit. The detailed systematic writing of this analysis is given in Ref. (7).

Continuing in parallel with the discussion of inelastic scattering we shall make the same fundamental assumption that there exists a transverse momentum cutoff at any strong vertex. Equation (35) says that the first thing that happens is the creation of a pion pair or of a proton-antiproton pair. In the limit of large q^2, energy momentum conservation forces at least one energy denominator in the expansion of U(0) in the old-fashioned perturbation series to be of order $q^2 \gg M^2$ or $k_\perp^2$ for diagrams involving interactions between the two groups of particles, the one group created by one member of the pair and the other group created by

the other member of the pair produced by j_μ. Therefore contributions of these diagrams illustrated in Fig. 15 vanish as $q^2 \longrightarrow \infty$. Diagrams with different pairs created at the two electromagnetic vertices as in Fig. 15b also vanish by similar reasoning. In complete analogy to the scattering problem as discussed earlier, the state $U(0)|Pn\rangle$ may be treated as an eigenstate of the total Hamiltonian with eigenvalue $E_p + E_n$. Thus Eq. (35) can be written with the aid of the translation operators as

$$\overline{W}_{\mu\nu} = 4\pi^2 \frac{E_p}{M} \int (dx) e^{+iqx} \sum_n \langle 0|j_\mu(x)U(0)|Pn\rangle \langle nP|U^{-1}(0)j_\nu(0)|0\rangle \qquad (36)$$

A simple kinematical consideration reveals that most of the longitudinal momentum of the virtual photon is given to that particle in the pair produced from the vacuum by j_μ which will eventually create the detected proton of momentum $\underset{\sim}{P}$. As an example, consider the second order diagram with the pion current operating as in Fig. 16a (Fig. 16b is its parallel in the inelastic scattering). The contribution of this diagram to $\overline{W}_{\mu\nu}$ according to the charge symmetric γ_5 pion-nucleon canonical field theory model is

$$\overline{W}_{\mu\nu} = \frac{g^2}{(2\pi)^3} \frac{1}{2M} \int \frac{d^3P_{\bar{n}}}{2E_{\bar{n}}} \frac{1}{2\omega_-} \delta(q^o - E_p - E_{\bar{n}} - \omega_-) 4k_{+\mu} k_{+\nu} \frac{\mathrm{Tr}\left|(M-\gamma P)(M-\gamma P_{\bar{n}})\right|}{(2\omega_+)^2 (E_p + E_{\bar{n}} - \omega_+)^2} \qquad (37)$$

The notations used here are self-explanatory; in particular we use $q_3 = \frac{1}{w} P$ by (34). In terms of the momentum parametrizations indicated in Fig. 16, the

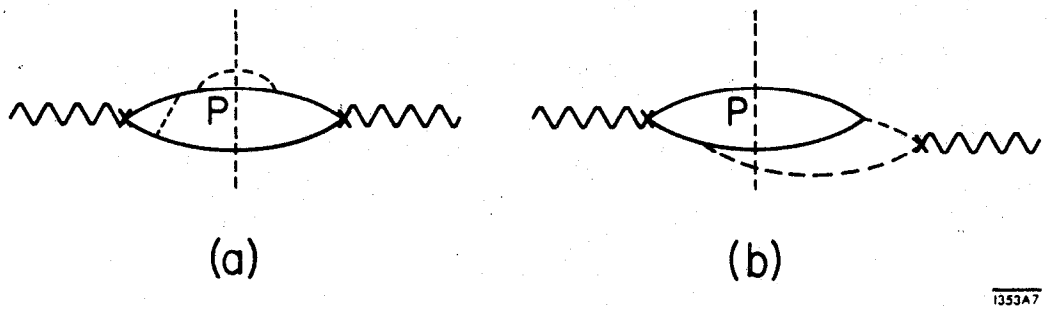

FIG. 15

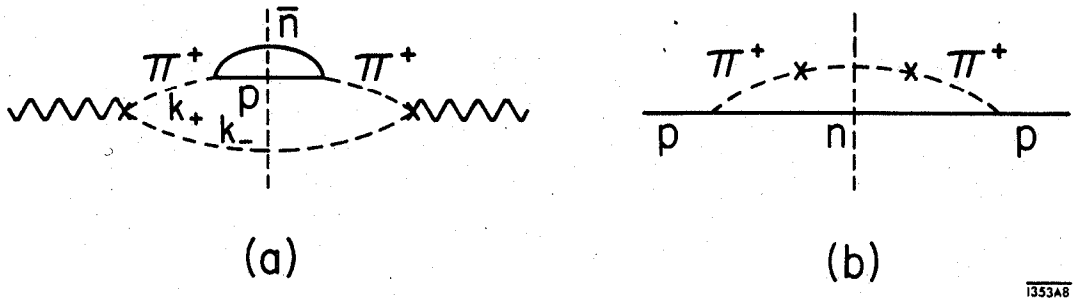

FIG. 16

solution to the energy conserving delta function in (37) is

$$\eta = \frac{1}{w} + \left(\frac{k_\perp^2}{2M\nu}\right) \longrightarrow \frac{1}{w} \text{ as } 2M\nu \to \infty$$

Hence by (34)

$$\underset{\sim}{k}_+ = \eta \underset{\sim}{P} + \underset{\sim}{k}_\perp = \underset{\sim}{q}_3 + \underset{\sim}{k}_\perp ,$$

and

$$\underset{\sim}{k}_- = \left(\frac{1}{w} - \eta\right)\underset{\sim}{P} - \underset{\sim}{k}_\perp \sim \left(\frac{k_\perp^2}{q^2}\right)\underset{\sim}{q}_3 - \underset{\sim}{k}_\perp$$

which verifies our assertion. Thus the virtual photon creates two distinct groups of particles with no interactions between the two. The group which contains the detected proton moves with almost all of the longitudinal momentum q_3, while the other group moves with a very small fraction $\sim(k_\perp^2/q^2)q_3$. Again the U matrix acts on the two groups separately and independently. We can sum over all possible combinations of particles in the small momentum group to obtain unity for the total probability for anything to happen. In other words, in Eq. (36) we have retained only those terms in which the small momentum group involves only one charged particle ($\pi^\pm$, P or $\bar{P}$) which we shall denote by λ. Therefore

$$\overline{W}_{\mu\nu} = 4\pi^2 \frac{E_p}{M} \int (dx) e^{+iqx} \sum_{n,\lambda=\pm} \langle 0 \left| j_\mu(x) \right| \lambda, U(0)(Pn) \rangle \langle (nP)U^{-1}(0), \lambda \left| j_\nu(0) \right| 0 \rangle \qquad (38)$$

which is the analogue of (23). As suggested by Fig. 16, in the Bjorken limit the same classes of diagrams contribute to eP scattering and annihilation processes.

Although it is not apparent that $\overline{F}_1(w)$ and $\overline{F}_2(w)$ computed from (38) are the same as $F_1(w)$ and $F_2(w)$ computed from (23) and continued to $0 < w \quad 1$, it is actually so by explicit calculation. Verification is trivial for second order pion current contributions and for the similar ones for nucleon current contributions of Fig. 16. In particular, (37) gives

$$\nu \overline{W}_2 = \frac{g^2}{8\pi^2} \frac{1}{w^2} \ell n \left[1 + \frac{k_{1\,max}^2}{M^2} \frac{1}{\frac{1}{w^2} + \frac{\mu^2}{M^2}\left(1 - \frac{1}{w}\right)} \right] \qquad (39)$$

We have also verified[7] this explicitly to fourth order in g for diagrams with both pion and nucleon current contributions, and to any order for ladder diagrams with the nucleon current operating (Fig. 17 and its corresponding diagram for the annihilation process). In this verification we only have to identify the transverse momentum cutoffs in both cases, viz. between Figs. 16(a) and (b) for the simplest example.

We can now study the experimental implications of (32). In the Bjorken limit, (30) becomes, using $E = M\nu/q^0 = M\nu/\sqrt{q^2}$ and the definition $w = \frac{2M\nu}{q^2}$

$$\frac{d^2\sigma}{dw\,d\cos\theta} = \frac{3}{2}\,\sigma_\ell \left[-F_1(w) + \frac{1}{4}\, w\, F_2(w)\, \sin^2\theta \right] w \qquad (40)$$

where

$$\sigma_\ell = \frac{1}{3}\,\frac{4\pi\alpha^2}{q^2}$$

is the total cross section of electron-positron annihilation into muon pairs, in the relativistic limit. Generally, knowledge about $F_{1,2}(w)$ for $w > 1$ as determined by inelastic e-p scattering measurements does not provide any useful information for $0 < w < 1$ unless one knows the analytic forms of $F_{1,2}(w)$ exactly. However $w = 1$ is a common boundary for both scattering and annihilation. Therefore with a mild assumption of smoothness the ep deep inelastic scattering data near $w \gtrsim 1$ predict completely the "deep" inelastic annihilation process near $w \lesssim 1$. This

connection is a far reaching consequence of the Bjorken limit. The two processes occur in different and disjoint kinematical regions and are not related in general. Recall that w = 1 corresponds to the two-body elastic channel and by w near 1 we still mean $|q^2(w-1)| \gg M^2$.

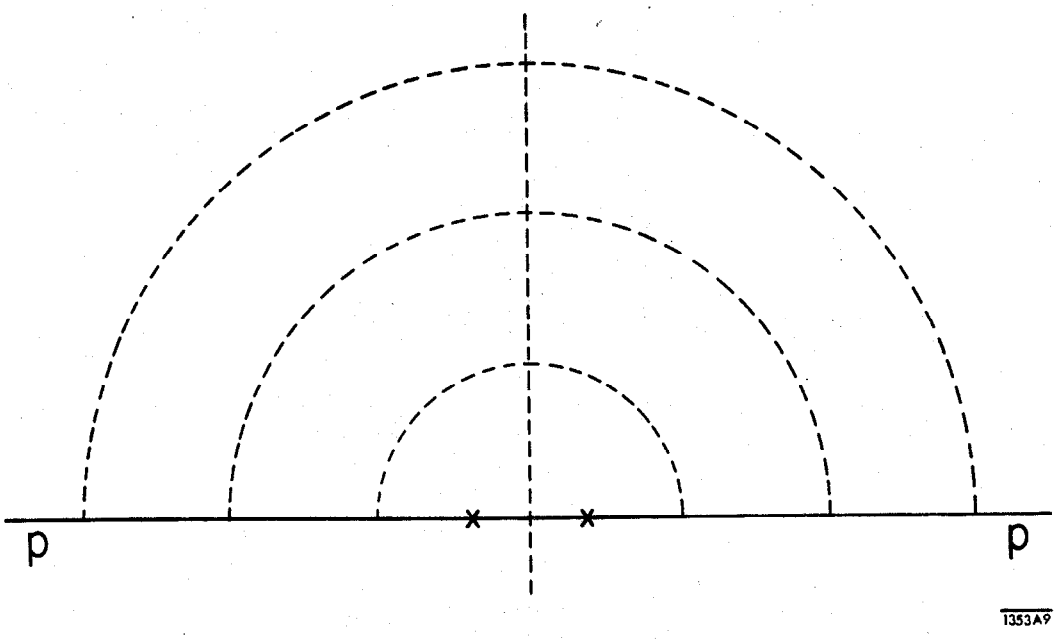

FIG. 17

In (40) we may choose $\sin^2\theta = 0$; thus it is necessary that

$$F_1(w) \leq 0, \quad 0 < w < 1 \tag{41}$$

It can be readily verified that for any value of w if the interaction of the current is with the nucleon

$$F_1(w) = \frac{w}{2} F_2(w); \quad j_\mu = \overline{\psi}_P \gamma_\mu \psi_P$$

and if it is with the pion

$$F_1(w) = 0; \qquad j_\mu = i\pi^+ \overleftrightarrow{\partial_\mu} \pi^-$$

On the other hand, $F_{1,2}(w)$ are non-negative for $w > 1$. We conclude that both $F_1(w)$ and $F_2(w)$ change sign at $w = 1$ if the nucleon current dominates, while $F_2(w)$ does not change sign at $w = 1$ if the pion current dominates. We therefore predict near $w \sim 1$ that

$$F_2(w) = C_N(w-1)^{2n+1}, \quad n = 0, 1, \ldots \quad \text{(Nucleon current)}$$

$$F_2(w) = C_\pi(w-1)^{2n}, \quad n = 0, 1, \ldots \quad \text{(Pion current)} \tag{42}$$

We are not able to perform a reliable calculation near $w \simeq 1$ from our field theoretical model, since the virtual particles involved are very virtual, and the off-shell effects must be correctly taken into account. This is in contrast to our results[7] for large $w \gg 1$ where we found the intermediate particles to be close to their energy shells and the vertex and self-energy corrections to contribute lower powers of $\ell n\, w \gg 1$ for each order of g^2. However, a plausible conjecture can be made. Diagrams without strong vertex corrections properly included indicate that the pion current gives the dominant contribution near $w \sim 1$. For example to lowest order in g^2 we find near $w \gtrsim 1$ from (39) for the pion current and from a similar expression for the nucleon current contribution that

$$F_2(w) \cong \frac{g^2}{16\pi^2}\, \ell n \left[1+k_\perp^2\, \max/\mu^2\right](w-1) \quad \text{(Nucleon current)}$$

$$F_2(w) \cong \frac{g^2}{8\pi^2}\, \ell n \left[1+ k_\perp^2\, \max/M^2\right] \quad \text{(Pion current)} \tag{43}$$

The virtual particle (a proton in the first case and a pion in the second) has a large (space-like) invariant mass proportional to $\frac{k_\perp^2}{w-1}$. If a form factor is included at each of the two pion-nucleon vertices as illustrated in Fig. 18 (43) becomes

$$F_2 \propto (w-1)\, F_P^2\left(\frac{c}{w-1}\right) \quad \text{(Nucleon current)}$$

$$F_2 \propto F_\pi^2\left(\frac{c'}{w-1}\right) \quad \text{(Pion current)} \tag{44}$$

The subscripts P or π at the squares of the pion-nucleon form factors indicate the particle which is virtual. If F_p and F_π behave similarly for large momentum transfers, then the pion current will continue to dominate with one less power of $(w-1)$ as $w \longrightarrow 1$ when the vertex corrections are included. On the basis of our conjecture we interpret $F_2(w)$ near $w \sim 1$ as a measure of the asymptotic pion-nucleon form factor.[12]

We want to emphasize that independent of this specific conjecture based on our model it follows from the existence of a Bjorken limit that the deep annihilation cross section varies with total energy of the colliding electron-positron system as $1/q^2$ just the same as the cross section for a point hadron. Furthermore even without calculating the specific values of $F_{1,2}(w)$ from a theory one can predict from (40) plus the observed structure functions for inelastic scattering that there will be a sizable cross section and many interesting channels to study in the deep inelastic region of colliding $e^- e^+$ beams. Moreover the distribution of secondaries in the colliding ring frame will look like two jets with typical transverse momenta $k_\perp \ll \sqrt{q^2}$ on the individual particles. The relative roles of the nucleon and pion currents can be studied by separating $F_1(w)$ from $F_2(w)$, or $\overline{W}_1$ from $\nu\overline{W}_2$ by the angular distribution in (40).

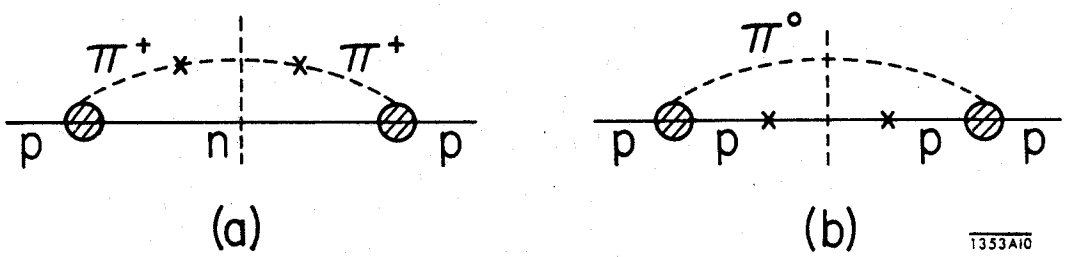

FIG. 18

Three further observations are worth noting:

1) By detecting different baryons in the final states one has a simple test of the unitary symmetry scheme of strong interactions. For instance, according to SU_3 and the hypothesis that the electromagnetic current is a U-spin singlet, the differential cross sections labeled by the detected baryon and observed at identical values of q^2 and $q \cdot P$ should satisfy the relations

$$\sigma_{\Xi^-} = \sigma_{\Sigma^-}, \quad \sigma_{\Sigma^+} = \sigma_P$$
$$\sigma_{\Xi^0} = \sigma_N = \frac{1}{2}(3\sigma_\Lambda - \sigma_{\Sigma^0}).$$

Similar relations can be written for the mesons with an added constraint due to the fact that π^- and π^+ are each others antiparticles; thus

$$\sigma_{\pi^-} = \sigma_{K^-} = \sigma_{\pi^+} = \sigma_{K^+}$$
$$\sigma_{K^0} = \sigma_{\bar{K}^0} = \frac{1}{2}(3\sigma_\eta - \sigma_{\pi^0}).$$

This should be an ideal place to test SU_3 relations since the mass differences among members of a multiplet should have a negligible effect on the dynamics as well as the kinematics in these regions of asymptotically large momentum and energy transfers.

2) If charge conjugation is a good symmetry of the electromagnetic interactions the differential cross sections for detecting a particle or its antiparticle are identical. According to (40) the differential cross section as a function of q^2 is comparable in magnitude to that for lepton pair creation and very much larger than the observed "elastic" annihilation process from a $p\bar{p}$ pair. Consequently it should be feasible by detecting and comparing charge-conjugate states, such as Λ and $\bar{\Lambda}$ for example, to test charge conjugation conservation in electromagnetic interactions of hadrons.[13]

3) Finally you may wonder what are the implications of this model and the existence of a Bjorken limit for $e^- e^+$ annihilation to form a deuteron (or any other "composite" system in place of the proton) plus anything. These are best illustrated by considering the deuteron and noting that the kinematically allowed regions are the same as illustrated in Fig. 14 but with the mass M now interpreted as the deuteron mass $M_D \approx 2M$. For inelastic scattering from the deuteron the very large proportion of the cross section comes from the kinematic region corresponding to one of the nucleons in the deuteron serving as a spectator and the other as the target — i.e., for $w_D \equiv \frac{2M_D \nu}{Q^2} > 2$. When we probe into the region $1 < w_D < 2$ which is also kinematically allowed we are simultaneously probing into very large momentum components of the deuteron wave function. To see this most directly we compute the invariant mass of the intermediate proton formed from the bound deuteron and moving in the infinite momentum center-of-mass frame for the deuteron plus incident electron as used in (10). The result by a straightforward calculation with the kinematics shown in Fig. 19 is

$$\mathcal{M}^2 - M^2 \approx - M^2 \left(\frac{(w_D \eta' - 2)^2}{w_D \eta' (w_D \eta' - 1)} \right) + \frac{4M\epsilon}{\eta' w_D}$$

where $0 < \eta' < 1$ is the fraction of longitudinal momentum of the intermediate proton

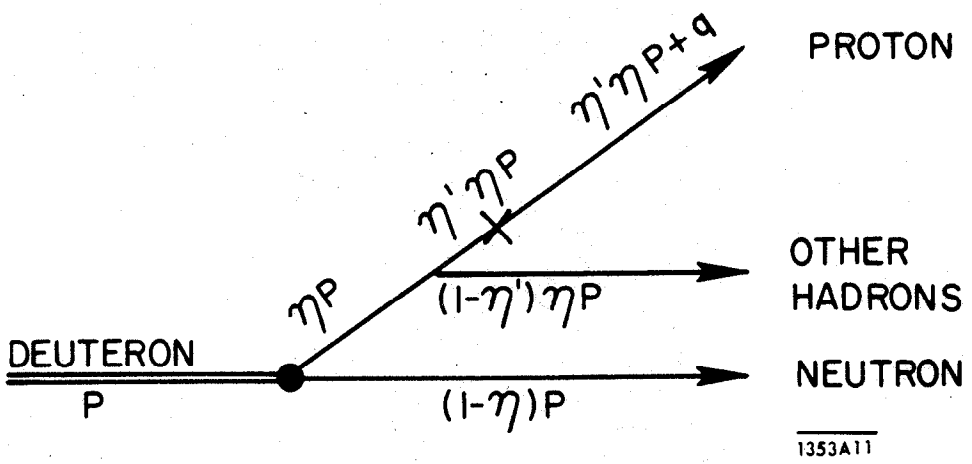

FIG. 19

retained on the final proton and $(1-\eta')$ is the fraction acquired by all the other hadrons produced from the proton. This shows that only for $w_D = 2/\eta' \geq 2$ are the low momentum components of the deuteron contributing so that the deuteron wave function does not severely damp the amplitudes νW_2 and W_1. In order to continue to the colliding beam region as we did for proton targets it would be necessary to continue across the boundary from $w_D > 1$ to $w_D < 1$. However once w_D decreases below $w_D = 2$ we have seen that the inelastic scattering is very severely dampened and hence we can expect the same very small cross section for deuteron production in $e^- e^+$ annihilation processes where $w_D < 1$.

This brings us to the end of these lectures. In a hurried and sketchy manner we have constructed a formalism for deriving the inelastic structure functions in the Bjorken limit — i.e., the "parton" model — from canonical field theory. To accomplish this derivation it was necessary to assume that there exists an asymptotic region in which the momentum and energy transfers to the hadrons can be made greater than the transverse momenta of their virtual constituents or "partons" in the infinite momentum frame.

In addition to deriving the inelastic scattering structure functions, we have accomplished the crossing to the annihilation channel and established the parton model for deep inelastic electron-positron annihilation. We found as an important consequence of this derivation that the deep inelastic annihilation processes have very large cross sections and have the same energy dependence, at fixed $w \equiv 2M\nu/q^2$, as do the point lepton cross sections.

REFERENCES AND FOOTNOTES

1. See Rapporteur's talk of W. K. H. Panofsky, Proceedings of the 14th International Conference on High Energy Physics, Vienna, (1968).
2. See reports by L. Hand and J. D. Walecka in the Proceedings of the 1967 International Symposium on Electron and Photon Interactions at High Energies, Stanford, California; cf. Ref. 1, (1967).
3. This is approximately true for high energies and small scattering angles. Kinematic corrections are known and can be made for the more general case. S. D. Drell and C. L. Schwartz, Phys. Rev. 112, 568 (1958).
4. R. P. Feynman (unpublished); J. D. Bjorken, Proceedings of the International School of Physics "Enrico Fermi," Course XLI, J. Steinberger, ed., (Academic Press, New York, 1968); J. D. Bjorken, E. A. Paschos, "Inelastic electron-proton and γ-proton scattering, and the structure of the nucleon," Report No. SLAC-PUB-572, Stanford Linear Accelerator Center, Stanford University, Stanford, California (1969).
5. J. D. Bjorken, Phys. Rev. 179, 1547 (1969).
6. See Ref. 1 and E. Bloom et al., Phys. Rev. Letters 23, 930 (1969); M. Breidenbach et al., ibid. 23, 935 (1969).
7. The following discussions are drawn from an analysis carried through in collaboration with Drs. Don Levy and Tung-Mow Yan at SLAC. Manuscripts of this work prepared for publication from the basis of these lectures. S. D. Drell, D. Levy, T.-M. Yan, Phys. Rev. Letters 22, 744 (1968).
8. L. Hand, Phys. Rev. 129, 1834 (1963).
9. H. Abarbanel, M. Goldberger, S. Treiman, Phys. Rev. Letters 22, 1078 (1969).
10. H. Harari, Phys. Rev. Letters 22, 1078 (1969).
11. S. Weinberg, Phys. Rev. 150, 1313 (1966).

12. On the other hand they are also consistent with $\sigma_\ell/\sigma_t \sim 0$ (< 0.2) near threshold suggesting by (19) and the above discussion that the nucleon and not the pion current dominates near $w = 1$. The relation of $F_2(w)$ near $w \sim 1$ and the large momentum transfer behavior of the elastic electromagnetic form factor has been discussed recently by Drell and Yan (SLAC-PUB-699) to be published.

13. If the baryon is built up of constituents or "partons" of spin 0 and 1/2 only with minimal coupling to the electromagnetic fields as in our model there is no possibility for C violation asymmetries to appear due to the restraints imposed by current conservation alone.